Batteries & Supercaps

Research Article
doi.org/10.1002/batt.202500177

Chemistry Europe
European Chemical Societies Publishing

www.batteries-supercaps.org

Systematic Study of Reactivity of Mg with Different Organic Solvents

Muath Radi, Nurbol Ibadulla, Cécile Courrèges, Alexandre Ponrouch,* and Rémi Dedryvère*

This study investigates the surface chemistry and reactivity of magnesium electrodes with various organic solvents to improve understanding of passivation layer formation and its impact on rechargeable magnesium batteries (RMBs). While Mg offers safety and sustainability advantages over lithium due to decreased dendrite formation and higher natural abundance, its performance is hindered by challenges such as passivation layers that impede Mg^{2+} conductivity. Using X-ray photoelectron spectroscopy and time-of-flight secondary ion mass spectrometry, we systematically studied Mg reactivity after immersion in ethers, alkyl and cyclic carbonates, esters, and nitriles investigating the composition of the formed passivation layer. With very short immersion, Mg surfaces develop a thin, uneven passivation layer which turns into a more uniform structure over time. Immersion in 0.1 M $Mg(TFSI)_2$/diglyme electrolyte revealed minimal salt degradation but led to $MgCO_3$ formation due to salt impurities. Contrary to prior findings, this study demonstrates that the solvent type and immersion duration significantly affect its chemical composition, while the passivation layer thickness increase remains limited upon time of immersion. By providing a detailed quantitative analysis of the Mg passivation process, this work bridges gaps in understanding Mg reactivity with organic solvents and contributes to the development of RMBs.

1. Introduction

Although Li-ion batteries (LIBs) based on graphite electrodes are among the most commercially widespread technologies for various applications, their energy density is limited due to the low theoretical capacity of graphite (372 mAh g^{-1}). While lithium metal is considered to be the holy grail negative electrode due to its huge theoretical capacity and low redox potential, with lithium plating and stripping occurring during charge and discharge, metallic lithium tends to form uneven deposits leading to dendrites and serious safety risks.[1]

Alternatively, rechargeable magnesium batteries (RMBs) are attractive due to their high gravimetric and volumetric capacities. Magnesium metal, with a low redox potential of –2.37 V versus standard hydrogen electrode (SHE), is less reactive and less prone to dendrite formation than lithium, enhancing safety and stability of the batteries. Moreover, magnesium is one of the most abundant elements in the Earth's crust (23.3 g kg^{-1}), which is around a thousand times more than lithium (20 mg kg^{-1}), making it a sustainable and cost-effective option for large-scale energy storage applications.[2,3]

However, the development of magnesium batteries faces two significant obstacles: First, the lack of suitable positive electrode materials. Mg^{2+} cations have a smaller ionic radius than Li^+ (0.72 vs. 0.76 Å) and carry a double charge.[4] This results in higher charge density for Mg^{2+}, leading to stronger coulombic interactions with the host material. Consequently, ion diffusion becomes sluggish. Second, by contrast with LIBs for which a solid electrolyte interphase (SEI) is usually formed on the negative electrode being electronically insulating and Li^+ conducting,[5] Mg electrodes in contact with organic electrolytes tend to form passivation layers that are not conductive for the Mg^{2+} cations.[6] Mitigation strategies include: 1) replacing Mg by a material with slightly higher operating potential (limiting electrolyte reduction) such as Mg alloys; 2) designing pre artificial Mg^{2+}-conducting interphase such as thermally cyclized polyacrylonitrile[7] or $MgSiN_2$, MgS, MgSe, $MgBr_2$, and MgI_2;[8] or 3) by developing more efficient electrolytes to improve the Mg plating/stripping reversibility and kinetics.[9] Besides, for high performance and practical applications, the electrolyte must be noncorrosive, nonflammable, nonvolatile with high ionic conductivity and enabling electrochemical plating and stripping of metallic magnesium with high Coulombic efficiency.[10]

While the surface chemistry of lithium electrodes in contact with organic solvents is rather well-understood, the surface state of magnesium electrodes remains incompletely explored. Gofer et al. systematically investigated magnesium electrodes in various organic solutions using X-ray photoelectron spectroscopy (XPS).[11] Their results indicated that there is no significant difference in the surface composition between the Mg samples exposed to different solvents and the pristine Mg. Only the sample in contact with PC showed a trace of carbonate formation. This experiment, conducted over a 2-month immersion period, was designed to study the effect of contact time. The conclusion

M. Radi, N. Ibadulla, C. Courrèges, R. Dedryvère
IPREM, E2S-UPPA, CNRS
Université de Pau & Pays de l'Adour
2, av. Pdt P. Angot, 64053 Pau, France
E-mail: remi.dedryvere@univ-pau.fr

A. Ponrouch
Solid State Chemistry Department
Institut de Ciència de Materials de Barcelona, ICMAB-CSIC
Campus UAB, 08193 Bellaterra, Spain
E-mail: aponrouch@icmab.es

Supporting information for this article is available on the WWW under https://doi.org/10.1002/batt.202500177

Research Article
doi.org/10.1002/batt.202500177
Chemistry Europe
European Chemical Societies Publishing

was that the different solvents have a minimal impact, and the duration of immersion has only a minor influence on the surface composition of the Mg samples.[11]

Nonetheless, the nature of the solvent being used has a profound impact onto the reversibility of metal Mg anode. The ether solvent family (mostly glymes) currently being the most effective one, enabling reversible plating and stripping. While different studies previously investigated the nature of the passivation layer formed onto Mg metal, such studies usually involve single electrolyte formulation and specific cycling history.[6]

In the present study, we extend this investigation by examining the reactivity of metallic magnesium with a large variety of organic solvents like ethers, alkyl and cyclic carbonates, esters, and nitriles through XPS analysis. Such study focuses on the formation of the native passivation layer (i.e., being formed before electrochemical test) in order to better understand the initial stage of the Mg interface before cycling. Furthermore, we examine the impact of contact duration on the reactivity between Mg and these solvents. We propose a comprehensive quantitative analysis of XPS data to reveal the detailed surface chemistry of the Mg passivation layers, aiming at improving our understanding of the passivation processes of the Mg electrode.

2. Results and Discussion

2.1. Pristine Mg Disk with its Native Passivation Layer

Figure 1a shows the XPS Mg 2p, C 1s, O 1s core peaks, and the Auger Mg KLL spectra of the unscratched Mg disk without using a flood gun. The Mg 2p core peak can be fitted with three components: The red one at the lowest binding energy (*B.E.*) of ≈49.7 eV represents metallic Mg which agrees with the standard reported value,[12] while the other two peaks at higher *B.E.* correspond to Mg^{2+} (as found, e.g., in compounds like MgO, $Mg(OH)_2$ or $MgCO_3$). The Mg KLL Auger spectrum also displays three peaks. The highest kinetic energy (*K.E.*) peak (on the right) reveals metallic Mg (*K.E.* ≈ 1186 eV), while the intermediate *K.E.* peak is due to Mg^{2+} (*K.E.* ≈ 1180 eV). The lowest *K.E.* peak (≈1175 eV) is due to both contributions (metallic Mg and Mg^{2+}). The C 1s spectrum can be fitted with four components, indicating the presence of carbon atoms in CH_x, CO, COO, and CO_3 environments. It is worth noticing a +1.7 eV shift to higher *B.E.* of these components; for example, the CH_x component appears at ≈286.7 eV instead of the expected 285 eV. This shift is due to the absence of charge compensation on the sample surface without using the flood gun (see the Supporting Information (SI) about surface charging effect). The characteristic components of metallic Mg (in Mg 2p and Mg KLL spectra) are not shifted since the samples are metallic conductors in electrical contact with the spectrometer. Only 1.6 at% of metallic Mg is detected in the surface composition of the sample from the Mg 2p spectrum because it is covered by a passivation layer. The O 1s spectrum comprises three components, also affected by charging effect. The small red peak at ≈531 eV is attributed to MgO, while the two green components correspond to a mixture of organic oxygenated species (CO, COO, and CO_3) and $Mg(OH)_2$. The quantitative data (**Table 1**) display the atomic percentages (at%) of chemical species based on *B.E.* assignments (taking the observed shifts into account). Note that only three elements are detected by XPS at the surface: Mg, C, and O (since H is not detectable by XPS). Therefore, oxygen can be associated only to Mg, C, and H. Association to C is clearly evidenced by the C–O, COO, and CO_3 components in C 1s spectra and allows to quantify the corresponding oxygen (including

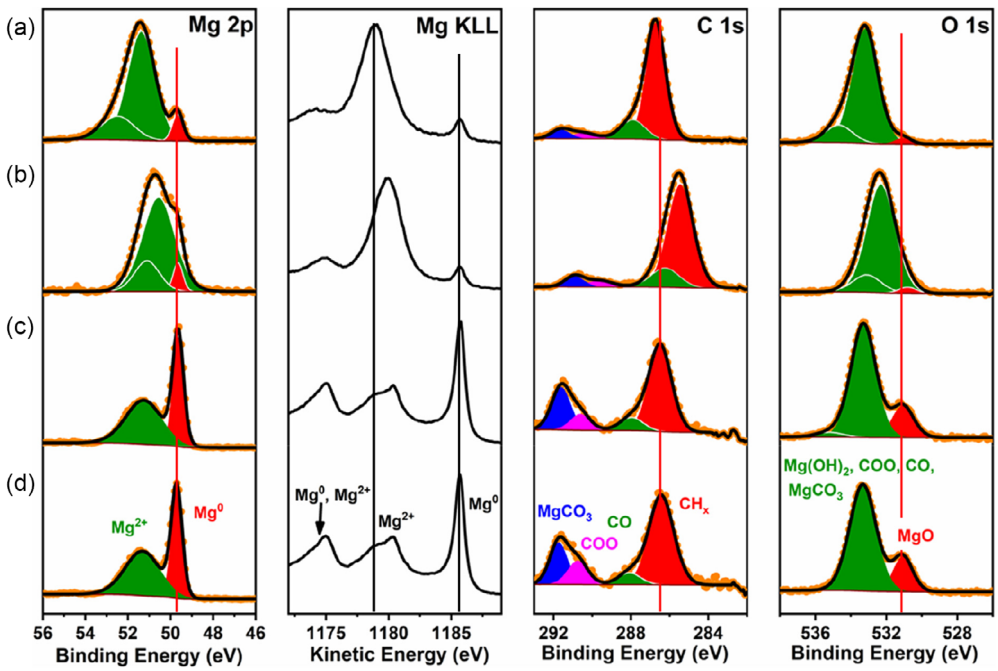

Figure 1. XPS Mg 2p, C 1s, and O 1s core peaks and Auger Mg KLL spectra of the unscratched Mg disk, a) without and b) with using the flood gun, and of the scratched Mg disk in the Ar atmosphere of the glovebox, c) without and d) with using the flood gun (no *B.E.* calibration was applied).

Table 1. Binding energy (*B.E.*) and atomic percentage (at%) of the components observed in XPS spectra reported in Figure 1.

Core peak	*B.E.* [eV] Figure 1a	*B.E.* [eV] Figure 1b	[at%]	*B.E.* [eV] Figure 1c	[at%] Figure 1c	*B.E.* [eV] Figure 1d	[at%] Figure 1d	
Mg 2p	49.7	49.7	1.6	49.6	19.2	49.7	19.1	Mg^0
Mg 2p	51.4	50.6	17.2	51.3	25.2	51.3	25.2	Mg^{2+}
Mg 2p	52.5	51.1	4.4					Mg^{2+}
C 1s	286.7	285.5	27.8	286.5	9.1	286.4	9.8	CH_x
C 1s	287.9	286.2	5.7	288.0	1.4	288.1	1.2	C–O
C 1s	290.5	289.6	1.8	290.6	1.5	290.8	2.1	O=C–O
C 1s	291.6	290.9	2.2	291.6	3.8	291.7	3.4	$MgCO_3$
O 1s	531.0	530.8	1.2	531.1	7.6	531.1	7.7	MgO
O 1s	533.2	532.3	33.0	533.3	30.9	533.3	31.4	MgO + organic oxygen + $Mg(OH)_2$
O 1s	534.7	533.1	5.3	535.2	1.4			

$MgCO_3$). According to the C 1s spectrum, there is 5.7 at% of carbon in CO environment, equating to $2 \times 5.7 = 11.4$ at% of CO groups (1 C + 1 O). Similarly, 2.2 at% of carbon in carbonate environment results in a global quantity of $5 \times 2.2 = 11$ at% of $MgCO_3$ (1 Mg + 1 C + 3 O) at the surface of the sample. By similar calculations, there is $3 \times 1.8 = 5.4$ at% of COO groups and $2 \times 1.2 = 2.4$ at% of MgO based on the O 1s spectrum. These quantities are obtained from the C 1s peaks and the first (red) peak of Mg 2p and O 1s. Other Mg 2p and O 1s (green) components provide complementary information. By subtracting the amount of oxygen associated to CO, COO, $MgCO_3$, and MgO from the total amount of oxygen of the sample (39.5 at%), we can conclude that 22.4 at% of oxygen is still not attributed. Similarly, by subtracting the amount of magnesium corresponding to MgO and $MgCO_3$ (as deduced from the quantification of O 1s and C 1s peaks) from the total amount of magnesium at +II oxidation state (green components in Mg 2p spectrum of Figure 1), we can conclude that 18.2 at% of Mg^{2+} of magnesium is still not attributed. Now, besides MgO and $MgCO_3$, we expect the possible presence of $Mg(OH)_2$ in the native passivation layer of the sample. Indeed, the potential sources of unassigned oxygen can be due only to the association of Mg to O or OH, i.e., MgO and $Mg(OH)_2$. However, if $Mg(OH)_2$ was the only unassigned oxygen compound, the O/Mg ratio corresponding to unassigned O and Mg would be equal to 2, which is not the case here. As a result, another interpretation of the surface chemistry of the sample should be examined. Actually, the O/Mg ratio is much closer to 1. This suggests that most of the remaining unattributed Mg^{2+} belongs to MgO and not to $Mg(OH)_2$. Indeed, it cannot be $MgCO_3$ which is perfectly identified from its C 1s peak. Therefore, from the ≈18 at% of still unattributed Mg^{2+}, ≈14 at% are actually associated to MgO, while only the remaining 4 at% correspond to $Mg(OH)_2$. Accordingly, 42% of the green O 1s peak area at *B.E.* ≈533 eV (corresponding to an oxygen amount of 14 at%) is assigned to MgO. Finally, this means that MgO leads to two different peaks in the same spectrum.

Now, the attribution of two different O 1s components with different *B.E.* to the same chemical species is not common in XPS and contradicts the most usual way of interpretation of XPS spectra based on the comparison of the observed chemical shifts with the values found in XPS databases. Since this phenomenon will be observed several times at the surface of Mg disks, we have developed a detailed argumentation for the observation of two different peaks for the same compound in the Supporting Information. Our interpretation is based on the differential charging effect phenomenon observed during an XPS experiment and is linked to the thickness of an insulating layer at the surface of a metallic conductor. This phenomenon is also briefly discussed in our recently published paper about parameters affecting magnesium plating/stripping kinetics in rechargeable Mg batteries.[13]

To confirm the presence of the differential charging effect, we analyzed the unscratched Mg disk with the flood gun on (Figure 1b) at the same analysis point as in Figure 1a. This allowed us to employ the same peaks' areas in both figures and observe the flood gun's impact on peak positions. Notably, the two oxidized magnesium (Mg^{2+}) peaks in Mg 2p (green) are shifted to lower *B.E.* when the flood gun is used, causing them to overlap more and become less distinguishable. Similarly, the largest peak in Mg KLL (assigned to Mg^{2+}) is shifted to a higher *K.E.* value (lower *B.E.*) after the flood gun is activated. All C 1s peaks also shift to lower *B.E.*, with the CH_x peak appearing at 285.5 eV (closer to the expected value of 285.0 eV) compared with the measurements without the flood gun. A similar shift to lower *B.E.* is also observed for the two large (green) peaks of O 1s. This behavior indicates that these surface species are not electronically conductive, contrary to the metallic Mg substrate, and the accumulated positive charges on them are neutralized by the flood gun's electrons. On the contrary, the metallic Mg signals in Mg 2p and Mg KLL are unaffected by the flood gun, maintaining the same binding energies (*B.E.* ≈ 49.7 eV for Mg 2p and *K.E.* ≈ 1185.7 eV for Mg KLL). Interestingly, the O 1s peak at 531 eV attributed to MgO (in red) does not shift and is unaffected by the flood gun. This suggests that this particular MgO component behaves similarly to metallic Mg in terms of charging effect. It implies that this MgO forms a "conductive" layer because very thin and in direct electrical contact with the Mg substrate, while the other MgO component, part of the main O 1s peak, corresponds to an MgO that is not in direct electrical contact with the metallic Mg (because of its greater thickness), as indicated by its shift to lower *B.E.* Additionally, it is important to note that the *B.E.*

difference between the Mg^0 peak in Mg 2p and the "conductive" MgO peak in O 1s (red peak) is consistently 481.3 ± 0.1 eV in both cases (with or without the flood gun). Similarly, the difference between the CH_x peak of C 1s and the main Mg^{2+} peak in Mg 2p remains at 235.2 ± 0.3 eV in both scenarios.

Figure 1c,d shows the same spectra of the scratched Mg disk without and with the flood gun, respectively. In these spectra, Mg 2p and Mg KLL exhibit a prominent peak corresponding to metallic Mg (≈19 at%), which is about 12 times higher than the detected Mg before scratching the passivation layer. The peaks assigned to Mg^{2+} in Mg 2p and Mg KLL have a distinctive shape compared to the prescratching state, which reveals a different surface composition. The C 1s spectrum is fitted with four peaks, similar to Figure 1a,b, but there is a noticeable decrease in the quantity of carbon in CH_x environment (≈10 at%) due to the scratching of the Mg disk's surface. The O 1s spectrum shows the same components as before scratching, but there is a significant increase in the MgO component at 531 eV, which can be correlated with the increased detection of the underlying metallic Mg and with the distinctive shape of Mg^{2+} signal of Mg KLL. Remarkably, all components of Mg 2p, Mg KLL, C 1s, and O 1s do not change whether the flood gun is used or not (i.e., the *B.E.* of all these peaks remain constant). Furthermore, all these peaks, except for the metallic Mg peaks in Mg 2p and Mg KLL, are observed at a higher *B.E.* compared to the expected value (+1.5 eV). It is important to remind that the *B.E.* is referenced to the Fermi level of magnesium since these conductive samples are in electrical contact with the spectrometer. The fact that the insulating passivation layer is insensitive to the flood gun means that it is thin enough to allow the positive charges resulting from photoemission to be completely neutralized by electron tunneling from the substrate (see Supporting Information about the influence of electron tunneling on surface charging effect). Additionally, it is sufficiently thin to let any excess negative charges formed on the surface by the flood gun to drain away to the substrate.[14] This explains why the flood gun does not affect the spectrum. Furthermore, this indicates that the +1.5 eV *B.E.* shift of the peaks attributed to the passivation layer cannot be explained by the differential charging effect as previously discussed in Figure 1a for the unscratched Mg disk. However, regardless the observed *B.E.* shift, the difference between the *B.E.* of the CH_x peak of C 1s and the Mg^{2+} peak in Mg 2p remains 235.2 eV in both scenarios in Figure 1c,d. This *B.E.* difference is similar to the one observed for the Mg disk before scratching (Figure 1a,b), indicating that they are neither dependent on the thickness of the passivation layer nor on the use or absence of the flood gun. The +1.5 eV *B.E.* shift of the core peaks of the scratched Mg disk's passivation layer, which cannot be explained by the charging effect, is likely correlated with the work function of the sample (Φ_{SA}). As an example, it has been reported that the *B.E.* of the C 1s peak of adventitious carbon (AdC) measured with respect to the Fermi level of a series of transition metal nitride thin films depends on the substrate, especially on the sample work function (Φ_{SA}). For instance, the *B.E.* of AdC varies from 284.08 eV for MoN to 285.52 eV for HfN samples.[15] In another study, it was found that for numerous thin film samples, including metals, nitrides, carbides, borides, oxides, and oxynitrides, the measured *B.E.* of the C 1s peak of AdC correlates well with Φ_{SA}, with the sum of both (*B.E.* + Φ_{SA}) being nearly constant at 289.58 ± 0.14 eV.[16] This means that a smaller Φ_{SA} results in a larger shift to a higher *B.E.* of the C 1s peak of AdC. Additionally, it was observed that the CH_x environment of AdC appears at different *B.E.* values, from 286.6 eV on the surface of Al foil to 285.0 eV on the surface of Au foil, which was also explained by the different Φ_{SA} of the two metal foils.[17,18]

To sum up this section, the XPS measurements disclose the surface chemistry of the unscratched and scratched Mg disk which is composed of a MgO, $MgCO_3$, $Mg(OH)_2$, and adsorbed organic species containing CH_x, CO, and COO groups but with different quantities. Furthermore, the XPS spectra of an unscratched Mg disk showed *B.E.* shifts due to differential charging effects which is mitigated by using a flood gun. Scratching the Mg disk revealed a significant increase in the detection of covered metallic Mg and MgO, and a +1.5 eV shift in the passivation layer's peaks, which is attributed to the sample's work function rather than charging. Note that it is important to consider all these complex phenomena to fully understand the surface chemistry of the samples.

2.2. Mg-Solvents Reactivity

Figure 2 presents the Mg 2p, C 1s, and O 1s core peaks and Auger Mg KLL spectra of a scratched Mg disk within different solvents. The data compare two immersion durations: 2 min and 60 days, showing how the interaction between the Mg surface and the solvents evolves over time. The Mg 2p and Mg KLL signals of metallic Mg appear at the same *B.E.* and *K.E.*, respectively, for all samples (Mg Fermi level as reference). The detection of the metallic Mg signal across all samples suggests that the passivation layer remains very thin in all cases (less than 10 nm, which is within the probing depth[19]). This thinness implies that the passivation layer does not significantly thicken over the immersion period and that the surface species that form on the Mg samples effectively prevent most spontaneous reactions between the active Mg and the solvents (i.e., they act as a passivation layer). Still, some differences in the shape of the Mg^{2+} component in Mg KLL spectra (*K.E.* ≈ 1180 eV) can be observed between 2 min and 60 days.

The C 1s spectra reveal the presence of several carbon environments on the Mg disk surfaces. The main peaks are associated with CH_x, CO, and COO groups. As a general observation, the C 1s spectra of samples measured after 2 min often show two peaks corresponding to the CH_x environment, except for the diglyme solvent, which only displays one peak. In the other samples, one peak is consistent with the expected *B.E.* of ≈285 eV, while the other one is shifted to a higher *B.E.* This shift can be attributed to the inhomogeneous thickness of the passivation layer on the sample surface (as discussed earlier for the native oxide layer of the Mg disk), with some regions covered by a much thinner passivation layer than other ones. In regions with a thinner passivation layer, the CH_x component of C 1s spectra is insensitive to the flood gun; moreover, it is shifted to higher *B.E.* due to the work function of the sample, as discussed earlier. Conversely,

Research Article
doi.org/10.1002/batt.202500177
Chemistry Europe
European Chemical Societies Publishing

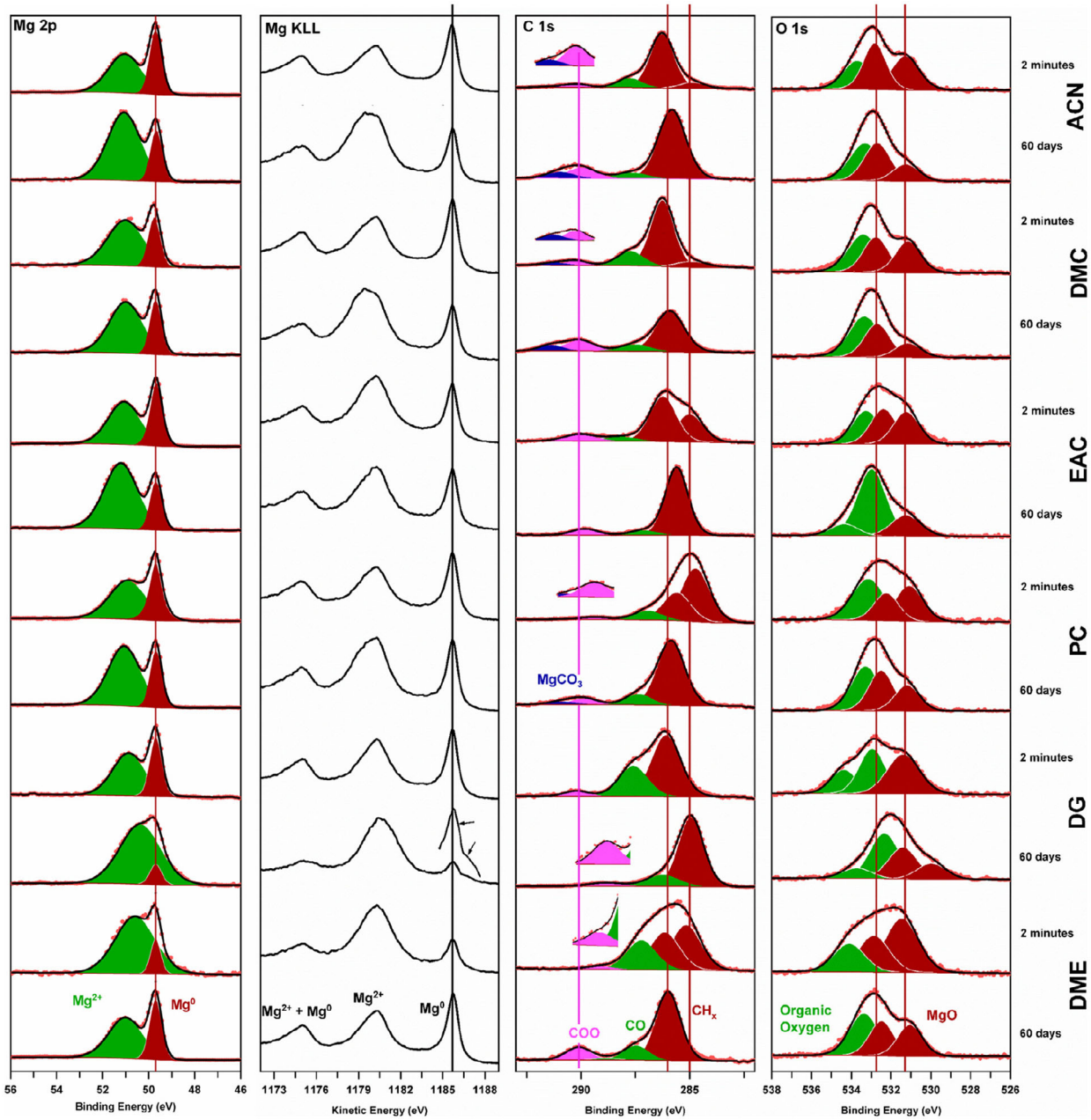

Figure 2. XPS Mg 2p, C 1s, and O 1s core peaks, and Auger Mg KLL spectra of the scratched Mg disk after immersion for 2 min and 60 days in DME, DG, PC, EAC, DMC, and ACN solvents in the Ar atmosphere of the glovebox (flood gun was used; no *B.E.* calibration was applied).

in samples areas with a thicker passivation layer, the response to the flood gun is more effective, resulting in a *B.E.* closer to the expected value.

After 60 days of immersion in the solvents, all samples exhibit a single C 1s peak corresponding to the CH_x environment, indicating a more homogeneous passivation layer in terms of thickness. This suggests that prolonged contact between Mg and the solvents leads to a more uniform passivation layer. So, in this work, the CH_x component is observed in a *B.E.* range from 284.7 to 286.5 eV depending on the thickness of the layer. The thicker layer shows lower *B.E.* closer to the expected value (285 eV).

It is worth mentioning that the *B.E.* difference between the CH_x peak of C 1s appears at the higher *B.E.*, and the Mg^{2+} peak in Mg 2p remains equal to 235.0 ± 0.3 eV in all samples in Figure 2. This value aligns well with those determined in the section devoted to the native passivation layer, whether before or after scratching, and regardless of a flood gun being used or not. This indicates that despite any *B.E.* shifts of the CH_x component, the *B.E.* difference between the CH_x and Mg^{2+} peaks in Mg 2p remains constant. The sample scratched in dimethoxyethane; monoglyme (DME) for 2 min shows the largest deviation from this value (235.6 eV), which can be attributed to the imperfections in the fitting of the C 1s peak, due to its particular unresolved shape.

Research Article
doi.org/10.1002/batt.202500177
Chemistry Europe
European Chemical Societies Publishing

The interpretation of the O 1s peak is supported by the quantification of the different oxygenated carbonaceous species based on the fitting of C 1s spectra, as explained in the previous section. To do this, we first subtract the amount of oxygen associated with CO, COO, and $MgCO_3$ (if present) from the total amount of oxygen detected in the O 1s spectrum. The remaining oxygen is then attributed either to MgO or $Mg(OH)_2$, since no extra source of oxygen is identified. Similarly, we subtract the amount of Mg^{2+} associated with $MgCO_3$ from the total amount of magnesium at +II oxidation state. The remaining Mg^{2+} is then assigned to MgO, $Mg(OH)_2$, or magnesium in an organic oxygen environment (such as CO or COO). By performing these calculations, we observe that in all samples, the remaining oxygen and Mg^{2+} have a 1:1 ratio, which strongly suggests the presence of MgO rather than $Mg(OH)_2$. In some instances, the remaining amount of Mg^{2+} is greater than the remaining amount of oxygen, indicating that there are MgO, and an additional remaining Mg^{2+} which cannot be associated with MgO, $Mg(OH)_2$, or $MgCO_3$ because there is no more remaining oxygen. This suggests that this additional Mg^{2+} is associated with organic oxygen environments (CO_x), i.e., to oxygen already considered in the quantification. As previously discussed, the two peaks observed for MgO arise from the differential charging effect. The peak at ≈531.3 eV is attributed to MgO in direct electrical contact with metallic Mg, while the higher *B.E.* peak (ranging from 532.2 to 533.9 eV) corresponds to MgO that is isolated from the metallic Mg (due to its thickness). In the sample scratched by DG and immersed for 60 days, an additional O 1s peak appears at ≈530 eV. We believe this additional peak is associated with a different form of metallic Mg, which is evident when looking at the Mg KLL Auger spectrum (see arrows in Figure 2), which reveals two different peaks for metallic Mg. This could be explained by the presence of small metallic Mg particles which are electrically disconnected from the rest of the Mg disk, after the scratching process with the stainless-steel spatula. Since the energy difference between the additional O 1s peak and additional metallic Mg KLL peak (*B.E.* O 1s + *K.E.* Mg KLL) remains constant, our conclusion is that the additional O 1s peak is attributed to a MgO layer covering this "second" metallic Mg.

Table S1 (Supporting Information) lists the atomic percentages for each element with the chemical attributions of each XPS component. From this quantification table, we can deduce the estimated atomic percentages of identified chemical species, like MgO and $MgCO_3$. To do so, the contributions of all atoms participating in the composition of one species are considered (e.g., at% $MgCO_3$ = at% Mg + at% C + at% O, which is equivalent to $MgCO_3 = 5 \times$ at% $C_{(CO3)}$). These calculated atomic percentages of the identified chemical species are shown in the stacked bar **Scheme 1**.

$MgCO_3$ is detected in samples treated with acetonitrile (ACN), dimethyl carbonate (DMC), and propylene carbonate (PC). The formation of $MgCO_3$ in DMC and PC samples is well expected based on our knowledge from Li system since these carbonate solvents can undergo a two-electron reduction on the surface of metallic Mg, resulting in the production of $MgCO_3$.[20] Trace water can also react with $(ROCO_2)_2Mg$ to form $MgCO_3$.[21,22] However, the presence of $MgCO_3$ in the ACN-scratched sample is not expected because there is no identified mechanism for carbonate formation from ACN. This implies that the $MgCO_3$ in ACN may have formed due to contamination in the solvent. For both ACN and DMC samples, a significant decrease in the amount of detectable metallic Mg is observed after 60 days of immersion (≈6 at% for both), compared to the 2 min (≈11 and 13 at%, respectively). This decrease is due to an increased surface coverage by $MgCO_3$ (≈12 at% for both) and organic species containing carboxylic groups (COO) (13 and 16 at%, respectively). The data indicate that prolonged exposure to these two solvents leads to the growth of a more substantial layer of magnesium carbonate and organic species containing carboxylic groups, which obscures the underlying metallic Mg. However, this does not result in any significant change in the amount of MgO (≈38–40 at%).

Similarly, in the EAC-treated sample, the amount of detectable metallic Mg also decreases after 60 days. This decrease is associated with an increase in the amount of the carbon species on the surface, particularly those containing CH_x and O–C=O functional groups. Interestingly, the amount of MgO decreases from 37 at% to 8 at% after prolonged exposure to EAC,

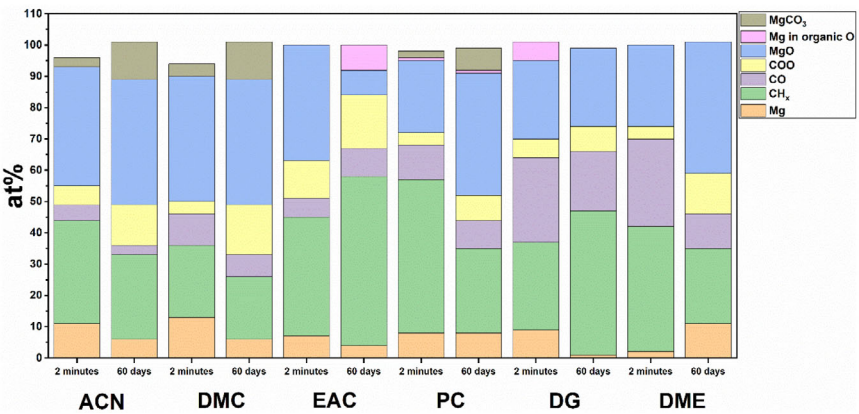

Scheme 1. Atomic percentage (at%) of some of the chemical species observed in XPS spectra reported in Figure 2 and Table S1 (Supporting Information) of the scratched Mg disk in the Ar atmosphere of the glovebox after immersion for 2 min and 60 days within the different solvents.

suggesting that some Mg^{2+} ions (≈8 at%) may be linked to organic oxygen. The decrease in the amount of MgO would be related with the less detectable metallic Mg and MgO as the thickness of the passivation layer grew with longer immersion time. Contrariwise, the PC sample experiences an increase in the amounts of MgO (39 at%), $MgCO_3$ (7 at%), and COO (8 at%) after 60 days of immersion, while the CH_x component decreases from 49 at% to 27 at%. Despite these changes, the overall amount of detectable metallic Mg remains relatively stable, indicating that the passivation layer does not necessarily grow in thickness upon immersion time but its composition evolved.

In the diethylene glycol dimethyl ether; diglyme (DG) solvent, there is a dramatic decrease in the detection of metallic Mg, from 9 at% to 1 at%, after 60 days. The surface becomes increasingly covered by carbon species, which may originate from reaction of the surface with the solvent. Initially, after 2 min, some Mg^{2+} is associated with organic oxygen (6 at%), but after 60 days, all Mg^{2+} appears as MgO.

Finally, in the DME-scratched sample, the reaction with the Mg disk leads to the formation of 26 at% of MgO, which increases to 42 at% after 60 days. Organic species containing COO functional groups also rise from 4 at% to 13 at% over the same period of time. Notably, the amount of detectable metallic Mg also increases after 60 days, possibly due to the reduced contribution of CH_x and CO species (24 at% and 12 at%, respectively), allowing for better detection of the Mg beneath it.

To get a quantitative estimation of the passivation layer thickness increase between 2 min and 60 days, we used the following formula based on the Mg 2p peak intensity corresponding to the metallic magnesium

$$I = I_0 \cdot e^{-\frac{\Delta d}{\lambda \cdot \cos\theta}} \quad (1)$$

where I_0 is the XPS intensity of metallic Mg after 2 min of immersion, I is the XPS intensity of metallic Mg after 60 days of immersion, Δd is the thickness increase of the passivation layer between 2 min and 60 days, and λ is the inelastic mean free path of Mg 2p photoelectrons in the passivation layer. By assuming that the main constituent of the passivation layer is MgO, we can take the value of pure MgO, which is estimated at 3.2 nm according to TPP-2M model[19] and θ is the angle between the normal line to the sample's surface and the detector (0° in our case, so $\cos\theta = 1$).

By using this formula and the Mg 2p intensities reported in Table S1 (Supporting Information), we find that immersion in ACN, DMC, EAC, and PC solvents for 60 days leads to an increase of the passivation layer thickness of 1.2 to 2.6 nm. For DME, the layer thickness even decreases after 60 days. The greatest increase is observed for DG, with a thickness increase of 6.4 nm after 60 days. Actually, one would expect a more significant growth of the passivation layer after 2 months of immersion, with a total disappearance of the metallic Mg 2p signal. This is not the case, and thus our conclusion is that the passivation layer thickness increase remains limited upon time of immersion.

Simultaneously and under the same condition of the experiment in Figure 2, Mg disk was scratched and immersed for 2 h and 5 days in the different solvents for better understanding the effect of intermediate immersion times on the reactivity of Mg disks with the solvents. This analysis focused on three selected solvents with distinct functional groups: ACN, EAC, and DG as depicted in **Figure 3**, with corresponding quantification data provided in Table S2 (Supporting Information). The general characteristics of the XPS spectra for the various samples remain consistent with those observed in Figure 2. Key features include the presence of metallic Mg, MgO, organic oxygen (such as CO and COO), and $MgCO_3$, particularly in the ACN-scratched Mg samples. By utilizing the quantification data in Table S2 (Supporting Information), the atomic percentages of identified chemical species were calculated, as summarized in **Scheme 2**.

In the ACN-scratched samples, the immersion time does not significantly affect the composition of the degradation products. Most Mg^{2+} ions remain in the form of MgO and $MgCO_3$, regardless of how long the samples are immersed. The amount of organic components also stays fairly consistent across the four immersion periods, with the exception of COO, whose content is multiplied by more than two with extended immersion. Additionally, the amount of $MgCO_3$ steadily increases over time, rising from 3 at% after 2 min to 4 at%, 5 at%, and finally 12 at% after 2 h, 5 days, and 60 days, respectively.

For the EAC-scratched samples, the highest amount of MgO is observed after 2 min of immersion (37 at%). However, this amount decreases significantly with longer immersion times, dropping to 4 at%, 14 at%, and 8 at% after 2 h, 5 days, and 60 days, respectively. On the contrary, more Mg^{2+} cations are bound to organic oxygen as immersion time in the EAC solvent increases (≈6–8 at%).

Finally, for the DG-scratched samples, immersion in the solvent for 2 h and 5 days results in a substantial increase in the amount of Mg^{2+} cations bound to organic oxygen (11-12 at%). However, after 60 days of immersion, all the Mg^{2+} cations are present in the form of MgO (25 at%). Notably, the amount of MgO is higher at both very short immersion times (2 min) and very long immersion times (60 days), reaching 25 at%. In contrast, during moderate immersion times (2 h and 5 days), the amount of MgO significantly decreases to around 11–12 at%. According to literature, glymes are supposed to be stable, but they were found to decompose when OH^- groups are present at the Mg metal surface.[23]

These results highlight the dynamic nature of the passivation layer that forms on the metallic Mg surface. Additionally, the findings suggest that various passivation species have different affinities for solubility in specific solvents. For instance, in the case of lithium, computational calculations indicated that compounds like $[\text{-}CH_2OCO_2Li]_2$ and $LiOCO_2CH_3$ are more soluble in ethylene carbonate (EC) than Li_2O and Li_2CO_3. This difference in solubility can influence the composition and stability of the passivation layer in different solvent environments.[24] Applying this conclusion to the Mg system, it could explain why Mg is found in an organic oxygen environment during the moderate immersion periods of 2 h and 5 days in DG solvent. However, after 60 days, this Mg environment is no longer observed, while the existence of a large amount of MgO is detected. In other words, over extended immersion periods, the less soluble passivation species, like MgO, dominate the surface composition, while the more

Research Article
doi.org/10.1002/batt.202500177
Chemistry Europe
European Chemical Societies Publishing

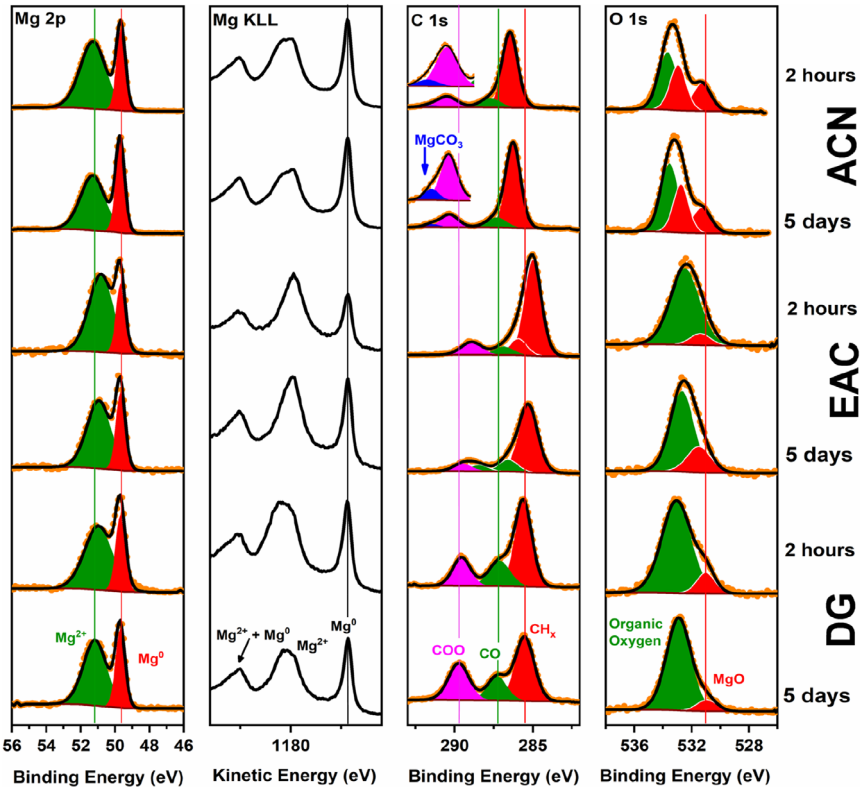

Figure 3. XPS Mg 2p, C 1s, and O 1s core peaks and Auger Mg KLL spectra of the scratched Mg disk in the Ar atmosphere of the glovebox after immersing for 2 h and 5 days with DME, DG, PC, EAC, DMC, and ACN solvents with using the flood gun (no *B.E.* calibration was applied).

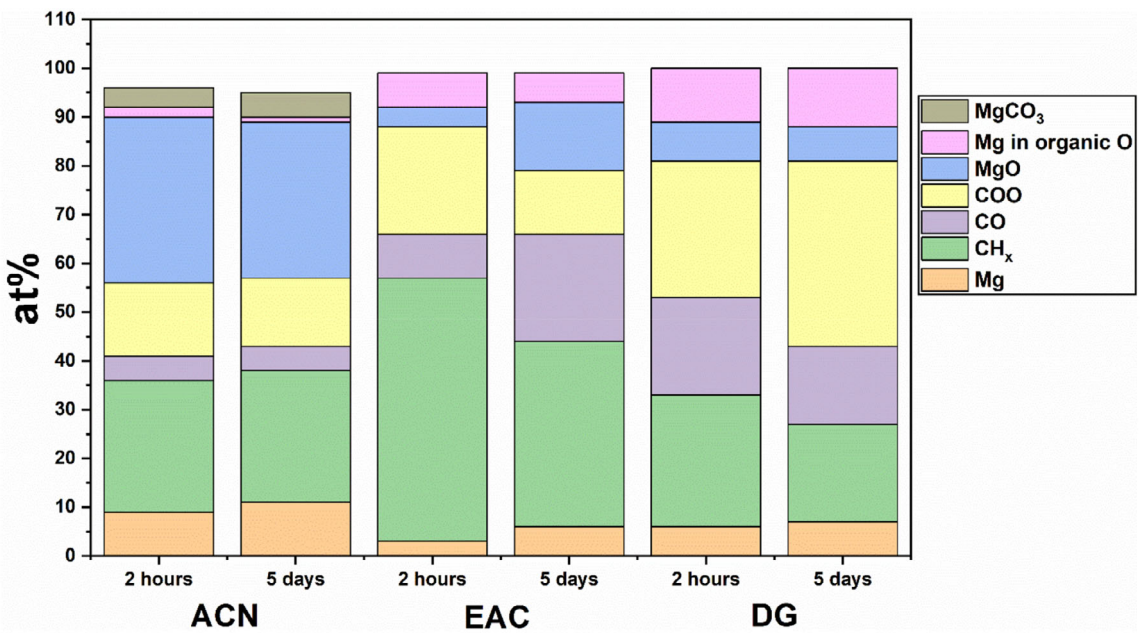

Scheme 2. Atomic percentage (at%) of some of the chemical species observed in XPS spectra reported in Figure 3 and Table S2 (Supporting Information) of the scratched Mg disk in the Ar atmosphere of the glovebox while immersion for 2 h and 5 days within the different solvents.

soluble organic species may dissolve into the solvent or undergo further reactions.

Scanning electron microscopy and nuclear magnetic resonance are not suitable characterization techniques to analyze few nm thick passivation layers on a metallic substrate. Therefore, complementary time-of-flight secondary ion mass spectrometry (ToF-SIMS) analysis was conducted on the surface of Mg deposits derived from the three scratched Mg samples

Research Article
doi.org/10.1002/batt.202500177
Chemistry Europe
European Chemical Societies Publishing

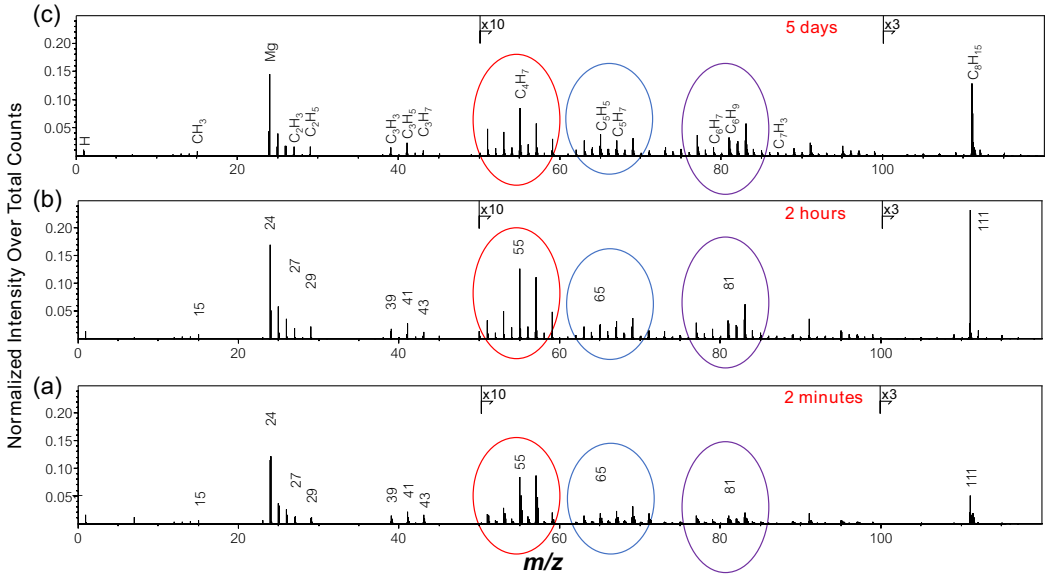

Figure 4. ToF-SIMS positive ion spectra over 0–120 m/z range for the scratched Mg disk in the Ar atmosphere of the glovebox after immersing for a) 2 min, b) 2 h, and c) 5 days with DG solvent.

after immersion for 2 min, 2 h, and 5 days in DG solvent as illustrated in **Figure 4**. This figure displays the ToF-SIMS positive ion spectra over the 0–120 m/z range. The detected secondary ions include m/z = 23.99 (Mg^+) and carbonaceous species such as m/z = 24.00 (C_2^+), m/z = 29.04 ($C_2H_5^+$) m/z = 29.00 (CHO^+), m/z = 41.04 ($C_3H_5^+$), m/z = 43.05 ($C_3H_7^+$), m/z = 43.02 ($C_2H_3O^+$), m/z = 55.05 ($C_4H_7^+$), m/z = 55.02 ($C_3H_3O^+$), m/z = 65.04 ($C_5H_5^+$), m/z = 79.05 ($C_6H_7^+$), and m/z = 87.03 ($C_7H_3^+$), originating from the solvent decomposition.

Notably, there is an intense peak at m/z = 111.1 which can be attributed to $C_6H_{15}Mg^+$ or $C_8H_{15}^+$. This peak is more intense in the samples immersed for 2 h and 5 days than in the 2-min sample. This observation correlates with the increased presence of organic peaks in the three spectral regions highlighted by ellipses in Figure 4, which further indicates that the 2-h and 5-day samples contain a higher concentration of organic species than the 2-minute sample. To confirm this further, Figure S1 (Supporting Information) presents the ToF-SIMS positive ion spectra over a higher m/z range (150–500) for the three samples, to highlight the presence of higher molecular weight organic species (e.g., oligomers or polymers). As a conclusion, these results are consistent with XPS observations that with moderate immersion time (2 h and 5 days), the Mg passivation layer composition is enriched in organic species.

2.3. Mg-Electrolyte Reactivity

Since DG is one of the most commonly used solvents in RMBs, particularly with $Mg(TFSI)_2$ salt, an additional experiment was conducted to study the reactivity of a Mg disk with the $Mg(TFSI)_2$/DG electrolyte. **Figure 5** presents the Mg 2p, C 1s, O 1s, F 1s, S 2p, and N 1s core peaks and Auger Mg KLL spectrum for

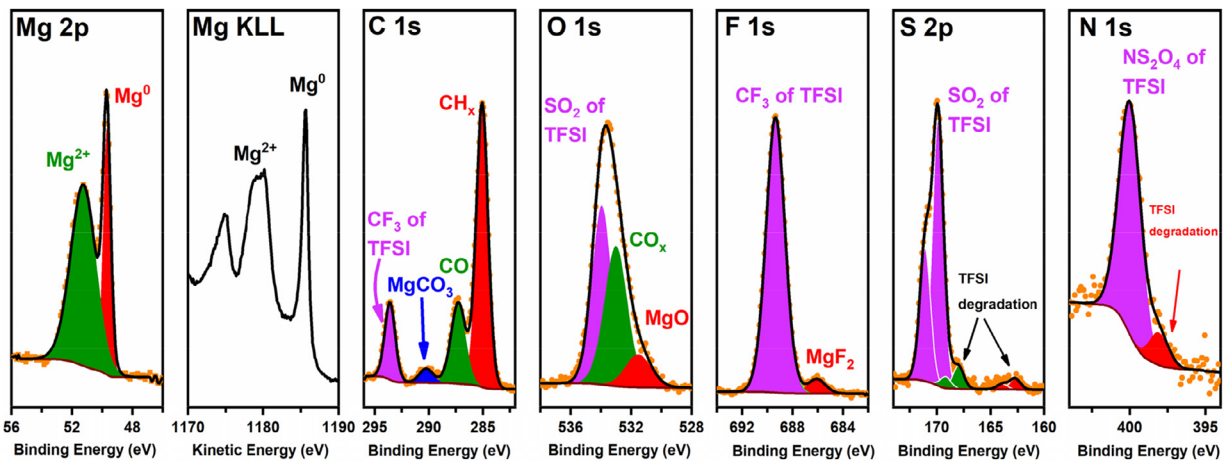

Figure 5. XPS Mg 2p, C 1s, O 1s, F 1s, S 2p, and N 1s core peaks, and Auger Mg KLL spectrum of the scratched Mg disk after immersion for 60 days in 0.1 M $Mg(TFSI)_2$ in DG electrolyte. (Flood gun was used, no *B.E.* calibration was applied).

a scratched Mg disk immersed for 60 days in a 0.1 M $Mg(TFSI)_2$/DG electrolyte. As shown earlier in Figure 2 and 3, the metallic Mg signals in the Mg 2p and Mg KLL spectra appear at the same *B.E.* and *K.E.*, respectively, referenced to the Mg Fermi level. The detection of metallic Mg indicates that the passivation layer remains very thin (<10 nm), implying minimal growth over the immersion period. This thin layer effectively prevents extensive spontaneous reactions between the active Mg and the electrolyte, thereby serving as a protective passivation layer. However, the addition of $Mg(TFSI)_2$ influences the composition of the passivation layer. For instance, the C 1s spectrum reveals multiple carbon environments on the Mg disk surface, such as CH_x and CO, consistent with observations from DG samples in Figure 2 and 3. Notably, two additional peaks at 290.2 and 293.6 eV correspond to $MgCO_3$ and $Mg(TFSI)_2$, respectively. The presence of $MgCO_3$ cannot be attributed to DG solvent degradation, as it was not observed in the DG samples in Figure 2 and 3. Instead, its formation appears to result from impurities in the $Mg(TFSI)_2$ electrolyte, as the salt's chemistry does not support a direct mechanism for $MgCO_3$ formation.

Salt degradation is demonstrated by the S 2p spectrum, which shows reduced sulfur species at 168.0 and 162.7 eV (representing S $2p_{3/2}$). Similarly, the F 1s spectrum reveals the presence of MgF_2 (≈2%, as quantified from Table S3 (Supporting Information)). The N 1s spectrum also shows a minor red peak at 398.1 eV, indicating salt reduction (which could lead to the break of an N–S bond, and the formation of CF_3-SO_2-N^{2-} species). Nevertheless, the overall salt degradation remains limited, as evidenced by the detection of the underlying metallic Mg substrate (from Mg 2p and Mg KLL signals) and the minimal quantities of the degradation products.

3. Conclusion

This study reveals that the reactivity of Mg disks with various solvents is significantly influenced by the duration of immersion, leading to distinct alterations in the chemical composition and passivation layers on the Mg surface. Initially, after 2 min of scratching in the solvents, a thin and inhomogeneous passivation layer forms, as evidenced by the two peaks of CH_x in C 1s spectra. However, over time, a more homogeneous passivation layer develops, particularly in samples immersed for 5 and 60 days, indicating enhanced protection of the Mg surface. This homogeneity refers to the thickness of the passivation layer rather than its chemical composition.

For the ACN-scratched samples, the immersion time has a minimal effect on the composition of degradation products, with Mg^{2+} ions predominantly forming MgO and $MgCO_3$. The gradual increase in $MgCO_3$ suggests a slow but steady interaction with the solvent. In the EAC-scratched samples, the decrease in MgO content and the increase in organic oxygen-bound Mg^{2+} cations over time point to ongoing chemical interactions that lead to more complex surface compositions and/or increasing the passivation layer thickness results in less detectable MgO. The DG-scratched samples exhibit a significant change in the passivation layer composition from MgO to organic oxygen-bound Mg cations with moderate immersion times, but return to a predominantly MgO composition after prolonged immersion in the solvent. Investigating Mg reactivity with 0.1 M $Mg(TFSI)_2$/DG electrolyte reveals very limited salt degradation and the formation of a thin passivation layer. Notably, the addition of $Mg(TFSI)_2$ to the DG solvent leads to the formation of $MgCO_3$, attributed to impurities in the electrolyte.

These findings highlight the dynamic nature of the interactions between Mg and various solvents, showing the importance of immersion time in determining the surface composition of Mg. Consistently with the literature,[11] our results confirm that the passivation layer thickness increase remains limited with extended immersion time in the solvent. However, in our systematic study, by exploiting the quantification data, we clearly demonstrate that both the nature of the solvent and the immersion time significantly affect the chemical composition of the passivation layers on Mg disks after scratching, which contradicts the conclusion of the previous research.[11] Our work contributes to a deeper understanding of the passivation layer on Mg electrodes and helps bridging the knowledge gap regarding Mg reactivity with organic solvents and electrolytes.

Finally, this study provides an analysis of the surface chemistry of the Mg disk and its native passivation layer exploring various phenomena, such as differential charging effects, that could influence XPS measurements and their interpretation. The insights gained from this paper highlight the impact of solvent choice on the surface chemistry of metallic Mg electrodes, which is critical for enhancing battery performance.

4. Experimental Section

Mg-Solvent Reactivity

To study the reactivity of metallic Mg with different organic solvents, Mg disks were completely immersed in the organic solvents and scratched with a stainless-steel flat spatula for two minutes inside the argon-filled glovebox, ensuring direct contact between metallic Mg and the solvent without interaction with glove box atmosphere. After scratching, the Mg disks were either immediately transferred for XPS analysis or left immersed in the organic solvent for various periods: two hours, five days, or 60 days and then transferred for the XPS analysis. Excess of solvent were removed by placing the samples onto previously dried soft tissues using capillarity effect and avoiding direct contact between the paper and the Mg surface later to be analyzed.

The solvents used in this investigation included:

Acetonitrile (ACN), 99.8% anhydrous, Sigma Aldrich.

Dimethyl carbonate (DMC), ≥99.9% anhydrous, Sigma–Aldrich.

Ethyl acetate (EAC), 99.8% anhydrous, Sigma–Aldrich.

Propylene carbonate (PC), 99.7% anhydrous, Sigma–Aldrich.

Diethylene glycol dimethyl ether, diglyme (DG), 99.5% anhydrous, Sigma–Aldrich.

Dimethoxyethane; monoglyme (DME), 99.5% anhydrous, inhibitor-free, Sigma–Aldrich.

Before using these solvents, they were purified over molecular sieves (3 Å from Alfa Aesar) for a minimum of three days and then analyzed

using a Metrohm 899 Karl-Fisher Coulometer to ensure the water content was lower than 2 ppm.

Finally, to investigate the reactivity between Mg and the complete electrolyte, a scratched Mg disk was immersed in 0.1 M magnesium bis(trifluoromethanesulfonyl)imide ($Mg(TFSI)_2$, 99.5% purity, Solvionic) dissolved in DG for 60 days in an Ar-filled glovebox. After immersion, the disk was recovered, washed with dry DG, and left to dry in the glovebox for a few hours before being transferred for XPS analysis.

XPS Analysis

Two metallic Mg disks (99.98%, Mateck) were mounted on copper conductive double-sided tape, ensuring electrical contact with the XPS spectrometer, thus allowing the use of the Mg Fermi level as a reference for binding energies. To enhance the signal of metallic Mg, one of the Mg disks was scratched on both faces with a stainless-steel flat spatula for 2 min under an argon atmosphere in a glovebox (O_2, $H_2O < 1$ ppm). This scratching process exposed the shiny metallic Mg beneath the native passivation layer. XPS measurements were performed using a Thermo Scientific ESCALAB 250 spectrometer equipped with an argon-filled glovebox directly connected to the introduction chamber, to maintain an inert atmosphere during preparation. The spectrometer utilized focused monochromatized Al Kα radiation ($h\nu = 1486.6$ eV), and the spectra were recorded at a pass energy of 20 eV and a 600 μm spot size. The measurements were conducted with and without charge compensation (flood gun). The analysis chamber pressure was maintained around 2×10^{-9} and 2×10^{-7} mbar while flood gun is off and on, respectively. Data fitting and analysis were carried out using CasaXPS software with the ESCALAB database's relative sensitivity factor (RSF).

ToF-SIMS Analysis

ToF-SIMS analysis was conducted using a TRIFT V Nano ToF II Tandem MS (Physical Electronics, Chanhassen, MN, USA) equipped with a 30 kV Bi_n^{q+}– LMIG (liquid metal ion gun) primary ion gun. Samples were transferred from the glove box to the spectrometer in a transfer vessel to avoid any exposure to air. The same conditions were maintained for all experiments, allowing for semi-quantitative analysis. The LMIG gun was configured to deliver Bi_3^{++} primary ions with an emission current of 0.5 μA over a $50 \times 50\ \mu m^2$ raster size. The m/z range was set between 0 and 1850, with the number of frames set to 30 (dose: 3.3×10^{12} ions/cm^2). For all analyses, charge compensation (with low dose of e^- and/or Ar^+) was applied to limit charging effects. ToF-SIMS data were processed using ToF-DR software (supplied by Physical Electronics). The positive polarity mass spectra were calibrated using C^+(m/z 12.00), CH^+(m/z 13.01), CH_2^+(m/z 14.02), CH_3^+(m/z 15.02) Mg^+(m/z 23.98), $C_2H_3^+$(m/z 27.02), and $C_2H_5^+$(m/z 29.04) peaks. For the graphical representation of spectra, the intensity of the secondary ions of interest was normalized related to the total ion counts.

Acknowledgements

R.D. thanks the French National Research Agency (STORE-EX Labex Project ANR-10-LABX-76-01) for financial support. A.P. gratefully acknowledges funding from the European Research Council (ERC) under the European Union's Horizon 2020 research and innovation programme (grant agreement no. 101089281) and the Spanish Agencia Estatal de Investigación Severo Ochoa Programme for Centres of Excellence in R&D (CEX2023-001263-S). M.R. acknowledges the European Union H2020-MSCA-COFUND Program for grant #945357 (DESTINY project) cofunded by University of Pau & Pays Adour.

Conflict of Interest

The authors declare no conflict of interest.

Data Availability Statement

The data that support the findings of this study are available from the corresponding author upon reasonable request.

Keywords: magnesium battery · metal anode · organic solvents · passivation layer · X-ray photoelectron spectroscopy

[1] X. B. Cheng, R. Zhang, C. Z. Zhao, Q. Zhang, *Chem. Rev.* **2017**, *117*, 10403.
[2] D. S. Tchitchekova, D. Monti, P. Johansson, F. Bardé, A. Randon-Vitanova, M. R. Palacín, A. Ponrouch, *J. Electrochem. Soc.* **2017**, *164*, A1384.
[3] L. Stievano, I. de Meatza, J. Bitenc, C. Cavallo, S. Brutti, M. A. Navarra, *J. Power Sources* **2021**, *482*, 228875.
[4] R. D. Shannon, *Acta Crystallogr. A* **1976**, *32*, 751.
[5] K. Xu, *Chem. Rev.* **2014**, *114*, 11503.
[6] J. D. Forero-Saboya, D. S. Tchitchekova, P. Johansson, M. R. Palacín, A. Ponrouch, *Adv. Mater. Interfaces* **2022**, *9*, 2101578.
[7] S. B. Son, T. Gao, S. P. Harvey, K. X. Steirer, A. Stokes, A. Norman, C. Wang, A. Cresce, K. Xu, C. Ban, *Nat. Chem.* **2018**, *10*, 532.
[8] T. Chen, G. Sai Gautam, P. Canepa, *Chem. Mater.* **2019**, *31*, 8087.
[9] J. Zhang, Z. Chang, Z. Zhang, A. Du, S. Dong, Z. Li, G. Li, G. Cui, *ACS Nano* **2021**, *15*, 15594.
[10] H. Zhang, L. Qiao, M. Armand, *Angew. Chem.* **2022**, *61*, e202214054.
[11] Y. Gofer, R. Turgeman, H. Cohen, D. Aurbach, *Langmuir* **2003**, *19*, 2344.
[12] J. F. Moulder, W. F. Stickle, P. E. Sobol, K. D. Bomben, J. Chastain, *Handbook of X-Ray Photoelectron Spectroscopy: A Reference Book of Standard Spectra for Identification and Interpretation of XPS Data*, Physical Electronics Division, Perkin-Elmer Corp., Waltham, MA **1992**.
[13] M. Radi, T. Purkait, D. S. Tchitchekova, A. R. Goñi, R. Markowski, C. Bodin, C. Courrèges, R. Dedryvère, A. Ponrouch, *Adv. Energy Mater.* **2024**, *14*, 2401587.
[14] G. Greczynski, O. Pshyk, L. Hultman, *Sci. Adv.* **2023**, *9*, eadi3192.
[15] G. Greczynski, L. Hultman, *Angew. Chem.* **2020**, *132*, 5034.
[16] G. Greczynski, L. Hultman, *Appl. Surf. Sci.* **2018**, *451*, 99.
[17] G. Greczynski, L. Hultman, *Sci. Rep.* **2021**, *11*, 11195.
[18] G. Greczynski, L. Hultman, *Appl. Surf. Sci.* **2022**, *606*, 154855.
[19] H. Shinotsuka, S. Tanuma, C. J. Powell, D. R. Penn, *Surf. Interface Anal.* **2015**, *47*, 871.
[20] A. N. Dey, B. P. Sullivan, *J. Electrochem. Soc.* **1970**, *117*, 222.
[21] D. Aurbach, N. Pour, in *Corrosion of Magnesium Alloys* (Ed: G. Song), Elsevier Inc., Amsterdam **2011**, pp. 484–515.
[22] Z. Lu, A. Schechter, M. Moshkovich, D. Aurbach, *J. Electroanal. Chem.* **1999**, *466*, 203.
[23] Y. Yu, A. Baskin, C. Valero-Vidal, N. T. Hahn, Q. Liu, K. R. Zavadil, B. W. Eichhorn, D. Prendergast, E. J. Crumlin, *Chem. Mater.* **2017**, *29*, 8504.
[24] K. Tasaki, S. J. Harris, *J. Phys. Chem. C* **2010**, *114*, 8076.

Manuscript received: March 10, 2025
Revised manuscript received: July 8, 2025
Version of record online: